

MULTIVARIATE WASSERSTEIN FUNCTIONAL CONNECTIVITY FOR AUTISM SCREENING

Oleg Kachan^{1,2} Alexander Bernstein³

¹ Laboratory for Algebraic Topology and Applications, HSE Univeristy

² Neuro Center, Skolkovo Institute of Science and Technology

³ AI Center, Skolkovo Institute of Science and Technology

ABSTRACT

Most approaches to the estimation of brain functional connectivity from the functional magnetic resonance imaging (fMRI) data rely on computing some measure of statistical dependence, or more generally, a distance between univariate representative time series of regions of interest (ROIs) consisting of multiple voxels. However, summarizing a ROI's multiple time series with its mean or the first principal component (1PC) may result to the loss of information as, for example, 1PC explains only a small fraction of variance of the multivariate signal of the neuronal activity.

We propose to compare ROIs directly, without the use of representative time series, defining a new measure of multivariate connectivity between ROIs, not necessarily consisting of the same number of voxels, based on the Wasserstein distance. We assess the proposed Wasserstein functional connectivity measure on the autism screening task, demonstrating its superiority over commonly used univariate and multivariate functional connectivity measures.

Index Terms— functional magnetic resonance imaging, fMRI, functional connectivity, optimal transport, clinical neuroscience

1. INTRODUCTION

Brain and its activity is a complex network consisting of neuronal populations, coactivity of which have to be consistent across large populations with individual differences and dependence on variables of interest such as age, socioeconomic status, and presence or absence of various neurodevelopmental and neurodegenerative diseases and conditions [1]. This activity known as the functional connectivity (FC), opposed to the structural connectivity which is the actual physical network of the neuronal populations and their interconnections, is estimated from the resting state functional magnetic resonance imaging (rs-fMRI).

Diseases and conditions are shown to be related to the increased, decreased, abnormal or generally altered functional connectivity, with the autism spectrum disorder (ASD) being prominent example. ASD is a condition related to the

brain development, which affects the individual's social behavior. ASD typically develops in infancy and early childhood and screened by the behavioral tests which may be subjective. Therefore, it is important to bring the quantitative, interpretable methods to screen autism, with fMRI being the promising modality to address that purpose.

The common approach to estimate FC consist of dividing the raw fMRI image time series into ROI groups defined by parcellation atlas. Next the representative time series of each ROI are obtained by averaging or principal component analysis (PCA), and some measure of dependence between each pair of representatives, most commonly the Pearson correlation coefficient is computed. We refer to this pipeline as the univariate approach, based on univariate time series representatives, assuming the homogeneity of the time series in each ROI.

Although as commonly raw time series are grouped into ROI based not on their similarity, but according to atlases based on neuroanatomy or brain's cytoarchitecture, one could not expect time series homogeneity within a ROI or single mode of their distribution. Recently introduced multivariate approach [1, 2, 3, 4] addresses this issue, with the most popular test for multivariate independence characterizing the relation strength is the distance correlation [5].

In our work we propose and assess a new multivariate measure of the functional connectivity based on the Wasserstein distance [6, 7] with the application to ASD screening.

2. MATERIALS AND METHODS

2.1. Functional connectivity

The functional connectivity is estimated from fMRI data using some measure of dependence between time series of each ROI, most often Pearson correlation coefficient between the representative time series of each ROI obtained by averaging or taking the first principal component.

More formally, given $\{X_i\}_{i=1}^N$ random variables with equal number of observations t , but of different dimensions $\{n_i\}_{i=1}^N$ where N is the number of ROIs, one seeks to estimate some measure of statistical dependence ρ_{ij} for each pair

(X_i, X_j) . If such estimating is done using 1-dimensional summaries of each X_i we call that *univariate* approach, otherwise if X_i and X_j are compared directly we call that *multivariate* approach.

2.1.1. Pearson correlation

Most often used similarity metric for comparing fMRI time series is *Pearson correlation*, which is defined for population as

$$\rho(X, Y) = \frac{\text{Cov}(X, Y)}{\sqrt{\text{Var}(X)\text{Var}(Y)}}. \quad (1)$$

Empirical Pearson correlation is given by

$$r(\mathbf{x}, \mathbf{y}) = \frac{\sum_{i=1}^n (x_i - \bar{x})(y_i - \bar{y})}{\sqrt{\sum_{i=1}^n x_i^2} \sqrt{\sum_{i=1}^n y_i^2}} \quad (2)$$

$$= \frac{\langle \mathbf{x}, \mathbf{y} \rangle}{\|\mathbf{x}\|_2 \|\mathbf{y}\|_2}, \quad (3)$$

with (3) valid for z-transformed vectors, standardized to the zero mean and unit variance.

2.1.2. Distance correlation

Pearson's correlation coefficient captures only linear association, with rank correlation coefficients traditionally used to address this issue. The relatively recently introduced distance correlation [5] in addition to being able to capture nonlinear dependencies is a multivariate measure of association between the groups of random variables of arbitrary, not of necessarily equal size. The idea of distance correlation is based on measuring the correlation of t^2 pairwise distances between realizations of random variables $X \in \mathbb{R}^n$ and $Y \in \mathbb{R}^m$, with population *distance correlation* is defined analogously to the Pearson correlation

$$dCor(X, Y)^2 = \frac{d\text{Cov}^2(X, Y)}{\sqrt{d\text{Var}^2(X)d\text{Var}^2(Y)}}. \quad (4)$$

For an observed random sample, given by the ROI matrices $\mathbf{X}, \mathbf{Y} = \{(X_k, Y_k) \mid 1, \dots, n\}$ from the joint distribution of random vectors $X \in \mathbb{R}^p$ and $Y \in \mathbb{R}^q$ define

$$\begin{aligned} a_{kl} &= |X_k - X_l|_p, \\ \bar{a}_{k.} &= \frac{1}{n} \sum_{l=1}^n a_{kl}, \quad \bar{a}_{.k} = \frac{1}{n} \sum_{l=1}^n a_{kl}, \quad \bar{a}_{..} = \frac{1}{n^2} \sum_{k,l=1}^n a_{kl} \end{aligned}$$

$k, l = 1, \dots, n$. to construct double centered pairwise distance matrix \mathbf{A} (and similarly for \mathbf{B}) with entries given by

$$(\mathbf{A})_{kl} = a_{kl} - \bar{a}_{k.} - \bar{a}_{.k} + \bar{a}_{..} \quad (5)$$

The empirical distance covariance $dCov_n(\mathbf{X}, \mathbf{Y})$ is defined by

$$dCov_n^2(\mathbf{X}, \mathbf{Y}) = \frac{1}{n^2} \sum_{k,l=1}^n A_{kl} B_{kl}. \quad (6)$$

The empirical distance variance $dVar_n(\mathbf{X})$ is defined by

$$dVar_n^2(\mathbf{X}) = \frac{1}{n} \sum_{k,l=1}^n A_{kl}^2. \quad (7)$$

Finally, the empirical *distance correlation* $dCor_n(\mathbf{X}, \mathbf{Y})$ is defined

$$dCor_n(\mathbf{X}, \mathbf{Y}) = \frac{dCov_n^2(\mathbf{X}, \mathbf{Y})}{\sqrt{dVar_n^2(\mathbf{X})dVar_n^2(\mathbf{Y})}}, \quad (8)$$

for $dVar_n^2(\mathbf{X})dVar_n^2(\mathbf{Y}) > 0$ and zero otherwise.

2.1.3. Wasserstein distance

Optimal transport considers comparing the measures over the domain X . Given a ground metric $d : X \times X \rightarrow \mathbb{R}$ optimal transport equips the space of measures $\mathcal{P}(X)$ with a metric referred to as the *Wasserstein distance* [6, 7], which for any $\mu, \nu \in \mathcal{P}(X)$ and $p \geq 1$ is defined as [8]

$$W_p^p(\mu, \nu) = \inf_{\pi \in \Pi(\mu, \nu)} \int_{X \times X} d^p(x, y) d\pi(x, y) \quad (9)$$

where W_p^p denotes the p -th power of W_p and $\Pi(\mu, \nu)$ is the set of probability measures on the product space $X \times X$ whose marginals coincide with μ and ν ; namely

$$\Pi(\mu, \nu) = \{\pi \in \mathcal{P}(X \times X) \mid P_1 \# \pi = \mu, P_2 \# \pi = \nu\}.$$

Given ROI matrices $\mathbf{X} \in \mathbb{R}^{n \times t}$ and $\mathbf{Y} \in \mathbb{R}^{m \times t}$, consider the discrete measures $\mu_{\mathbf{X}}, \nu_{\mathbf{Y}} \in \mathcal{P}(X)$ that can be written as linear combinations $\mu_{\mathbf{X}} = \sum_{i=1}^n a_i \delta_{\mathbf{x}_i}$ and $\nu_{\mathbf{Y}} = \sum_{j=1}^m b_j \delta_{\mathbf{y}_j}$ of Dirac's deltas centred at a finite number n and m of points $(\mathbf{x}_i)_{i=1}^n \in \mathbb{R}^t$ and $(\mathbf{y}_j)_{j=1}^m \in \mathbb{R}^t$. In order for μ and ν to be probabilities, set the vector weights $\mathbf{a} = (1/n, \dots, 1/n)^T \in \mathbb{R}^n$ and $\mathbf{b} = (1/m, \dots, 1/m)^T \in \mathbb{R}^m$.

We define the *Wasserstein functional connectivity (WFC)* as the Wasserstein distance between the two discrete measures $\mu_{\mathbf{X}}$ and $\nu_{\mathbf{Y}}$ with corresponding weight vectors \mathbf{a} and \mathbf{b} corresponds to

$$W_p^p(\mu_{\mathbf{X}}, \nu_{\mathbf{Y}}) = \min_{\mathbf{T} \in \Pi(\mathbf{a}, \mathbf{b})} \langle \mathbf{T}, \mathbf{M} \rangle_F, \quad (10)$$

where $\mathbf{M} \in \mathbb{R}^{n \times m}$ is the cost matrix with entries $(\mathbf{M})_{ij} = d^p(\mathbf{x}_i, \mathbf{y}_j)$ are set to the ℓ^p -distance $d^p(\cdot, \cdot)$, $\langle \mathbf{T}, \mathbf{M} \rangle_F$ is the elementwise Frobenius inner product, and $\Pi(\mathbf{a}, \mathbf{b})$ denotes the transportation polytope

$$\Pi(\mathbf{a}, \mathbf{b}) = \{\mathbf{T} \in \mathbb{R}_+^{n \times m} : \mathbf{T} \mathbf{1}_m = \mathbf{a}, \mathbf{T}^T \mathbf{1}_n = \mathbf{b}\}.$$

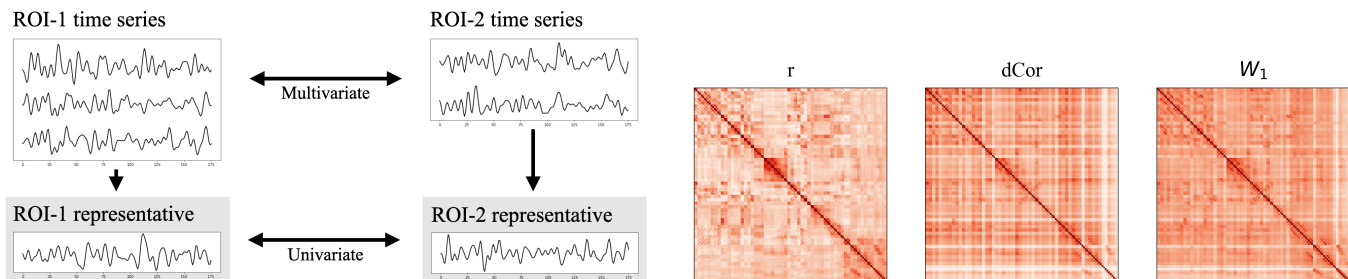


Fig. 1. Left: Computation of the functional connectivity. In the more common univariate approach a representative time series are computed for each ROI, for example by averaging or PCA and are compared. In the multivariate approach ROIs are compared directly, for example by distance correlation [5] or by the Wasserstein distance as in our proposal. **Right:** Mean connectivity matrices given by the Pearson and distance correlation and the Wasserstein distance. For the visualization matrices were transformed to have ones on the diagonal to facilitate the comparison.

2.2. Dataset

Autism Brain Imaging Data Exchange (ABIDE) [9] is a collaboration of 16 international imaging sites that have aggregated and are openly sharing neuroimaging data. The dataset is composed of structural and resting state functional MRI (rs-fMRI) data along with an extensive array of phenotypic information. We used the preprocessed version¹ with 879 subjects total, with 474 individuals suffering from ASD and 405 typical controls. Functional preprocessing was performed using the Configurable Pipeline for the Analysis of Connectomes (CPAC) including the band-pass filtering and global signal regression.

2.3. Experiment

Functional connectivity matrices were computed using the Pearson correlation between the ROI representative time series obtained by averaging, and the distance correlation in the voxel space and the Wasserstein distance in the time space for full ROIs. Being symmetric with the same values on the diagonal, matrices were further vectorized by taking the upper half triangle for each matrix.

Following the best practices in fMRI data analysis described in Dadi et al. [10], we used logistic regression with L1 and L2 regularization with the grid search for the regularization parameter on the $[0.2, 5]$ range. The data was split into the train and test subsets with the 80/20 ratio, with the random downsampling of the largest class performed to mitigate the class imbalance. The classification accuracy mean and standard deviation in percents for the best pair of the regularization norm and regularization parameter value averaged over 20 runs are reported in the Table 1.

Also we conducted the analysis of how considered connectivity measures are correlated between themselves. For that, first, mean connectivity matrices were computed for each measure, averaged for all subjects in the dataset. Second, the absolute differences between mean connectivity matrices of

the ASD-affected and control patients were computed. Then, for each set of matrices the correlation was computed for each pair in the set, summarizing the values for each pair in the Table 2.

3. RESULTS

	Univariate Pearson r	Multivariate dCor	Multivariate Wasserstein
All sites	64.09±0.00	62.95±0.00	65.54±0.00
Caltech	56.02±8.84	54.37±7.33	63.82±4.31
KKI	55.40±11.87	65.30±8.87	55.65±10.36
Leuven	59.05±5.58	68.60±5.37	59.42±9.02
MaxMun	55.88±11.17	80.14±4.23	63.18±7.10
NYU	62.96±3.35	58.51±3.02	64.32±3.68
OHSU	53.30±8.46	50.35±10.59	53.75±11.63
Olin	68.60±7.74	60.35±13.45	63.60±9.52
Pitt	70.67±3.70	66.92±5.89	73.04±5.41
SBL	60.55±6.73	48.55±8.16	68.00±12.08
SDSU	59.95±12.13	55.10±9.02	57.60±14.46
Stanford	58.88±6.12	93.57±2.95	97.07±0.17
Trinity	64.29±8.14	51.85±6.01	56.57±6.42
UCLA	64.74±3.36	50.04±5.29	65.34±3.05
UM	68.65±5.20	70.41±4.57	72.98±5.47
USM	65.66±4.27	64.43±6.46	69.81±5.21
Yale	69.43±9.02	56.35±6.26	64.76±8.04
Best	4/16	3/16	9/16
Avg. rank	2.06	2.50	1.44

Table 1. Comparison of the multivariate Wasserstein functional connectivity measure to the univariate and multivariate measures, represented by the Pearson and distance correlations respectively. Best classification accuracy, % for the ASD/control classification task is reported for the 5-fold cross-validation with 20 repeats on the ABIDE1 dataset. The three largest sites are emphasized by the **bold** font.

By the experimental evaluation on the ABIDE dataset –

¹<http://preprocessed-connectomes-project.org/abide/>

the benchmark for autism diagnosis, we obtained the following results:

- WFC outperforms the univariate and multivariate methods (Table 1) for the whole dataset composed of the data from all 16 sites.
- WFC is competitive sitewise, quantified by the best average rank, including being ranked first on the 3 largest sites – NYU (171 subjects), UM (82), USM (61). For the Stanford site using the WFC metric leads to mean accuracy increase of 38.19% compared to the Pearson correlation.
- WFC is more similar to dCor than to Pearson r , as shown with the visual inspection (Fig. 1, right) and high correlation between them obtained for the averaged connectivity matrices as reflected in the Table 2, despite WFC is being defined in the time space, not the voxel space contrary to dCor.

	r/dDcor	r/WFC	dCor/WFC
Mean	0.265	-0.584	-0.893
Difference	0.009	0.116	0.398

Table 2. Correlations between mean connectivity matrices computed using different connectivity measures and differences between ASD and control mean matrices.

4. DISCUSSION

Albeit shown to be beneficial for the downstream tasks, the main limitation of the Wasserstein distance connectivity measure is the increased computational complexity compared to both Pearson and distance correlations. This limitation can be addressed with several complementary approaches.

First is the use of dimensionality reduction – we observed that applying PCA on the time domain, taking 25% principal components with the subsequent computation of the Wasserstein distance does affect the value of WFC measure less than 1% for the worst case over the population. Second, one can replace exact computation of the Wasserstein distance with the computation-efficient approximations, making use of the entropic regularization [8] or tree metrics [11]. Third, while it is not affecting computational complexity, the computation of the connectivity matrix entries is independent of each other, so is amenable to the distributed and parallel computation.

The key suggestion that Basti et al. [4] make is that multivariate connectivity analysis benefits from increased functional inhomogeneity of time series constituting a ROI. The corresponding analysis of the dependence of the inhomogeneity and the performance of the classifiers using Wasserstein distance as connectivity measure relative to the univariate methods based on average and principal component analysis-based representatives is left for the future work.

Conclusions

We have proposed the new Wasserstein distance-based measure of the multivariate brain functional connectivity and demonstrated that it is preferable over the commonly used univariate and multivariate connectivity measures given by the Pearson and distance correlations respectively for the task of autism diagnosis.

5. COMPLIANCE WITH ETHICAL STANDARDS

This is a numerical simulation study conducted retrospectively using human subject data made available by Di Martino et al. [9] for which no ethical approval was required.

6. ACKNOWLEDGEMENTS

No funding was received for conducting this study. The authors have no relevant financial or non-financial interests to disclose.

7. REFERENCES

- [1] Linda Geerligs and Richard Henson, “Functional connectivity and structural covariance between regions of interest can be measured more accurately using multivariate distance correlation,” *NeuroImage*, vol. 135, pp. 16–31, 2016.
- [2] Alexander Walther, Hamed Nili, Naveed Ejaz, et al., “Reliability of dissimilarity measures for multi-voxel pattern analysis,” *NeuroImage*, vol. 137, pp. 188–200, 2016.
- [3] Kwangsun Yoo, Monica Rosenberg, Stephanie Noble, et al., “Multivariate approaches improve the reliability and validity of functional connectivity and prediction of individual behaviors,” *NeuroImage*, vol. 197, pp. 212–223, 2019.
- [4] Alessio Basti, Hamed Nili, Olaf Hauk, Laura Marzetti, and Richard Henson, “Multi-dimensional connectivity: a conceptual and mathematical review,” *NeuroImage*, p. 117179, 2020.
- [5] Gábor Székely, Maria Rizzo, and Nail Bakirov, “Measuring and testing dependence by correlation of distances,” *The Annals of Statistics*, vol. 35, no. 6, pp. 2769–2794, 2007.
- [6] Leonid Kantorovich and Gennady Rubinshtein, “On a space of totally additive functions,” *Vestnik of the St. Petersburg University: Mathematics*, vol. 13, no. 7, pp. 52–59, 1958.

- [7] Leonid Vaserstein, “Markov processes over denumerable products of spaces, describing large systems of automata,” *Problemy Peredachi Informatsii*, vol. 5, no. 3, pp. 64–72, 1969.
- [8] Gabriel Peyré, Marco Cuturi, et al., “Computational optimal transport,” *Foundations and Trends® in Machine Learning*, vol. 11, no. 5-6, pp. 355–607, 2019.
- [9] Adriana Di Martino, Chao-Gan Yan, Qingyang Li, et al., “The autism brain imaging data exchange: towards a large-scale evaluation of the intrinsic brain architecture in autism,” *Molecular Psychiatry*, vol. 19, no. 6, pp. 659–667, 2014.
- [10] Kamalaker Dadi, Gaël Varoquaux, et al., “Benchmarking functional connectome-based predictive models for resting-state fmri,” *NeuroImage*, vol. 192, pp. 115–134, 2019.
- [11] Tam Le, Makoto Yamada, Kenji Fukumizu, and Marco Cuturi, “Tree-sliced variants of wasserstein distances,” *Advances in Neural Information Processing Systems*, vol. 32, pp. 12304–12315, 2019.
- [12] Nathalie Tzourio-Mazoyer et al., “Automated anatomical labeling of activations in spm using a macroscopic anatomical parcellation of the mni mri single-subject brain,” *NeuroImage*, vol. 15, no. 1, pp. 273–289, 2002.
- [13] Rémi Flamary et al., “Pot: Python optimal transport,” *Journal of Machine Learning Research*, vol. 22, no. 78, pp. 1–8, 2021.